2018

Engineering Properties of Ambient Cured Alkali-Activated Slag-Fly Ash Concrete Reinforced with Different Types of Steel Fiber

Nabeel Farhan
University of Wollongong, naf010@uowmail.edu.au

M Neaz Sheikh
University of Wollongong, msheikh@uow.edu.au

Muhammad N. S Hadi
University of Wollongong, mhadi@uow.edu.au

Engineering Properties of Ambient Cured Alkali-Activated Slag-Fly Ash Concrete Reinforced with Different Types of Steel Fiber

Abstract

This paper investigates the influence of different types of steel fibers on the engineering properties of ambient cured alkali-activated slag-fly ash concrete. The engineering properties investigated include workability, compressive strength, splitting tensile strength, flexural strength, direct tensile strength, and stress-strain response under axial compression. Three types of steel fibers, i.e., straight micro steel fiber, deformed macro steel fiber and hybrid steel fiber, were added to the alkali-activated slag-fly ash mixes. It was found that the workability of the alkali-activated slag-fly ash concrete mixes decreased with the increase in the volume fraction of steel fibers. It was also found that the compressive strength, splitting tensile strength, flexural strength, and direct tensile strength of alkali-activated slag-fly ash concrete mixes increased with the addition of steel fibers. The stress-strain response of alkali-activated slag-fly ash concrete mixes changed from brittle to ductile by the addition of steel fibers. Significant improvements in the mechanical properties of alkali-activated slag-fly ash concrete were observed for the addition of 2% by volume of all three types of steel fiber. The addition of hybrid steel fiber (1% straight micro steel fiber plus 1% deformed macro steel fibers) showed the highest improvement in the mechanical properties of ambient cured alkali-activated slag-fly ash concrete.

Disciplines

Engineering | Science and Technology Studies

Publication Details

Farhan, N. A., Sheikh, M. Neaz. & Hadi, M. N. S. (2018). Engineering Properties of Ambient Cured Alkali-Activated Slag-Fly Ash Concrete Reinforced with Different Types of Steel Fiber. Journal of Materials in Civil Engineering, 30 (7), 04018142-1-04018142-12.

Engineering Properties of Ambient Cured Alkali-Activated Slag-Fly Ash Concrete Reinforced with Different Types of Steel Fiber

Nabeel A. Farhan[1]

[1] Ph.D. Candidate, School of CME Engineering, University of Wollongong, Australia.

Email: naf010@uowmail.edu.au

M. Neaz Sheikh[2]

[2] Associate Professor, School of CME Engineering, University of Wollongong, Australia.

Email: msheikh@uow.edu.au

Muhammad N. S. Hadi[3,*]

[3] Associate Professor, School of CME Engineering, University of Wollongong, Australia.

Email: mhadi@uow.edu.au, [*]Corresponding author

Abstract

This paper investigates the influence of different types of steel fibers on the engineering properties of ambient cured alkali-activated slag-fly ash concrete. The engineering properties investigated include workability, compressive strength, splitting tensile strength, flexural strength, direct tensile strength and stress-strain response under axial compression. Three types of steel fibers i.e., straight micro steel fiber, deformed macro steel fiber and hybrid steel fiber were added to the alkali-activated slag-fly ash mixes. It was found that the workability of the alkali-activated slag-fly ash concrete mixes decreased with the increase in the volume fraction of steel fibers. It was also found that the compressive strength, splitting tensile strength, flexural strength and direct tensile strength of alkali-activated slag-fly ash concrete mixes increased with the addition of steel fibers. The stress-strain response of alkali-activated slag-fly ash concrete mixes changed from brittle to ductile by the addition of steel fibers.

Significant improvements in the mechanical properties of alkali-activated slag-fly ash concrete were observed for the addition of 2% by volume of all three types of steel fiber. The addition of hybrid steel fiber (1% straight micro steel fiber plus 1% deformed macro steel fibers) showed the highest improvement in the mechanical properties of ambient cured alkali-activated slag-fly ash concrete.

Keywords: Alkali-activated; Ambient cured; Engineering properties; Strength; Steel fiber

Introduction

Rapid urbanization worldwide places a significant demand on infrastructure development. Increasing infrastructure development causes increasing demand of concrete and hence increasing demand of cement in the construction industry. Cement production is associated with the emission of greenhouse gases including carbon dioxide, methane and nitrous oxide into the atmosphere. It is estimated that the production of one ton of cement releases about 0.7 to 0.8 ton of carbon dioxide (CO_2) into the atmosphere (Peng et al. 2013). Hence, the need for alternative binders for reducing the carbon dioxide (CO_2) emissions is paramount. One of the possible solutions is to use industrial by-product materials as alternative binders to cement. Alkali-activated binder is considered as a promising alternative binder to cement. It is estimated that alkali-activated concrete emits about 26-45% less CO_2 than cement (Habert et al. 2011; McLellan et al. 2011). The alkali-activated binder has other advantages including better mechanical properties, better resistance to chemical attack, lower chloride diffusion and higher fire resistance than cement (Bakharev et al. 1999; Bakharev et al. 2003; Roy et al. 2000; Rashad et al. 2012).

Alkali-activated concrete can be prepared by using aluminosilicate materials such as fly ash (FA) and ground granulated blast furnace slag (GGBS). Alkali-activated concrete is obtained by activating an aluminosilicate material with a strong alkaline activator either at high temperatures or ambient conditions (Duxson et al. 2007). The chemical reaction and the strength development of alkali-activated concrete are influenced by several factors including chemical compositions of the aluminosilicate material, alkaline activators and curing conditions (Yip et al. 2008). Islam et al. (2014) observed that the compressive strength of alkali-activated concrete increased by increasing of GGBS content in the binder containing FA. The addition of GGBS with alkali-activated concrete achieved setting time and compressive strength equivalent to Ordinary Portland Cement (OPC) (Nath and Sarker 2014). Ryu et al. (2013) studied the effect of the chemical composition of alkaline activators on the compressive strength of alkali-activated concrete. The results showed that chemical composition of the alkaline activators had a significant influence on the early strength of the alkali-activated concrete.

The performance of alkali-activated concrete cured at high temperatures was investigated in recent research publications (Palomo et al. 1999; Bakharev 2005). These studies indicated that alkali-activated concrete achieved high compressive strength, high tensile strength and low porosity, which are beneficial for concrete in aggressive marine and corrosive environments. Fernandez-Jimenez et al. (2006) studied the mechanical properties of alkali-activated concrete and observed that alkali-activated concrete obtained comparable compressive strength, higher splitting and flexural tensile strengths, and lower modulus of elasticity than OPC concrete. Thomas and Peethamparan (2015) investigated the tensile strength, modulus of elasticity, Poisson's ratio, and stress-strain relationships of alkali-activated concrete made with FA or GGBS. Thomas and Peethamparan (2015) found that alkali-activated concrete obtained higher tensile strength and lower modulus of elasticity and Poisson's ratio than OPC concrete. Alkali-activated concrete was found to be more durable than conventional concrete in aggressive marine and corrosive environments (Olivia and Nikraz 2012). Most of the research studies on heat-cured alkali-activated concrete considered limited applications of alkali-activated concrete in the construction of precast concrete members. The development of alkali-activated concrete at ambient curing condition will increase its application in the construction of a wide range of structural members. The reduction in the CO_2 emissions, cost saving due to ambient curing and cast in-situ constructions are the main drivers for the development of ambient cured alkali-activated concrete (Hadi et al. 2017).

Although alkali-activated concrete possesses many desirable engineering properties, it lacks adequate ductility (Lokuge and Karunasena 2016). Moreover, alkali-activated concrete exhibits low tensile and flexural strengths (Shaikh 2013; Bhutta et al. 2017). However, the tensile strength, flexural strength and the ductility of the alkali-activated concrete can be enhanced by the addition of fibers. Fiber reinforced alkali-activated concrete was first investigated in Davidovits (1991). Afterwards, alkali-activated concrete with different types of fibers was investigated including carbon fiber (Ranjbar et al. 2015), polyvinyl alcohol fiber (Yunsheng et al. 2008), polypropylene fiber (Ranjbar et al. 2016) and steel fiber (Nataraja et al. 1999; Ng et al. 2013; Bernal et al. 2010). It was reported that the increase in the tensile and flexural strengths of alkali-activated concrete depends on the volume fraction, geometry and type of fibers. The addition of carbon fiber, polyvinyl alcohol fiber and polypropylene fibers in alkali-activated concrete are usually associated with poor fire resistance, poor bond with concrete and high sensitivity to sunlight and oxygen. A detailed literature review indicated that only a limited number of studies investigated the addition of steel fibers in heat cured alkali-activated concrete. Al-Majidi et al. (2017) investigated the effect of the addition of various type (steel, polyvinyl alcohol and glass) and various volume fraction (1%-3%) of fibers on the mechanical properties of alkali-activated concrete. It was found that the compressive strength of alkali-activated concrete improved significantly when 2% steel fibers by volume were added to the alkali-activated concrete mix. The use of hooked end and straight steel fibers (0.5%- 1.5%) improved the load carrying capacity, cracking strength, crack width and rate of crack growth in fiber reinforced heat cured alkali-activated concrete (Ng et al. 2013). Incorporation of steel fiber (0.5% and 1.5%) considerably improved splitting tensile strength and flexural strength of heat cured alkali-activated concrete (Bernal et al. 2010).

To the knowledge of the authors, none of the research studies investigated the addition of straight micro steel fibers, deformed macro steel fibers and hybrid steel fibers (combination of straight micro and deformed macro steel fibers) in ambient cured alkali-activated concrete. Also, none of the available studies investigated the direct tensile strength of alkali-activated concrete with different type of steel fibers. The direct tensile strength of the ambient cured alkali-activated concrete is significantly important for the analysis of the cracking and post-cracking response of reinforced concrete elements constructed with alkali-activated concrete. This study investigates the mechanical properties of ambient cured alkali-activated slag-fly ash concrete with straight micro steel fibers, deformed macro steel fibers and hybrid steel fibers. The objective of this study is achieved through extensive experimental studies. The investigation on the microstructural characteristics of the specimen using scanning electron microscope is considered beyond the scope of the paper.

Experimental details

Materials

Ground granulated blast furnace slag (GGBS) and fly ash (FA) were used as source materials to prepare the alkali-activated slag-fly ash concrete. The GGBS was supplied by the Australian (Iron & Steel) Slag Association (ASA 2017). The FA Classified as Class F according to ASTM C618-08 (ASTM 2012) was supplied by Eraring Power Station, Australia (EPSA 2017). The chemical compositions of the GGBS and the FA are reported in Table 1.

Crushed aggregate with a maximum size of 10 mm was used as coarse aggregate and river sand was used as fine aggregate. The alkaline activator consisted of combining sodium silicate (Na_2SiO_3) and sodium hydroxide (NaOH) solutions. The Na_2SiO_3 solution was supplied by PQ Australia (PQ 2017) with a specific gravity of 1.53 and an activator modulus (Ms) of 2.0 (Ms = SiO_2/Na_2O; SiO_2 = 29.4% and Na_2O = 14.7%). The sodium silicate (Na_2SiO_3) and sodium hydroxide (NaOH) solutions were blended for a Na_2SiO_3/NaOH mass ratio of 2.5. The amount of activator was 35% of the amount of binder. Hence, the amount of activator was 157.5 kg/m^3 (=0.35 × combined amount of fly ash and GGBS of 450 kg/m^3). The sodium hydroxide (NaOH) solution was prepared by dissolving the NaOH pellets in potable water. The mass of NaOH pellets varied depending on the concentration of the solution. For example, for preparing the NaOH solution with a concentration of 14 mole/l, 560 grams (14 pellets @ 40 grams = 560 grams) NaOH solid was mixed with potable water, where 40 is the molecular weight of NaOH. In order to mix the NaOH pellets with water, a magnetic stirrer was used. The mix was stirred until the pellets were fully dissolved in the water. The NaOH solution was prepared 24 hours before the mixing of concrete. The Na_2SiO_3 and NaOH solutions were blended together for a Na_2SiO_3/NaOH mass ratio of 2.5. In order to improve the workability, a commercially available high range water reducer, Glenium 8700, supplied by BASF, Australia was used.

In this study, three types of steel fibers were used, i.e., straight micro steel (MS) fibers, deformed macro steel (DS) fibers and hybrid steel (HS) fibers. The straight micro steel (MS) fibers were 6 mm in length and 0.2 mm in diameter. The nominal tensile strength of MS fibers was 2600 MPa. The DS fibers were 18 mm in length and 0.55 mm in diameter with a nominal tensile strength of 800 MPa. The HS fibers were a combination of MS fibers and DS fibers. The MS fibers were provided by Ganzhou Daye Metallic Fibers Company, China. The DS fibers were provided by Fibercon Company, Australia. Figure 1 shows the MS fibers and DS fibers.

Preparation of specimens

In the production of the alkali-activated slag-fly ash concrete, the component materials (GGBS, FA, coarse aggregate, and sand) were initially mixed in a pan mixer without steel fibers. The alkaline activators were prepared by combining Na_2SiO_3 and NaOH. High range water reducers and water were then added to the dry mix. Afterwards, the steel fibers were added gradually in order to avoid fiber balling and to produce an alkali-activated slag-fly ash concrete mix with reasonable workability. In this study, a total of three types of steel fibers with different volume fraction were used. The first type included 1%, 2%, and 3% by volume of MS fibers. The second type included 1%, 1.5% and 2% by volume of DS fibers. The third type included 2% by volume of HS fibers, which was a combination of 0.5% MS+1.5% DS fibers, 1% MS+1% DS fibers, and 1.5% MS+0.5% DS fibers. The weight of steel fiber with 2% by volume was equal to 7800 kg/m^3 $\times$ 0.02= 156 kg/m^3, where 7800 kg/m^3 is the density of steel fibers. Also, plain alkali-activated slag-fly ash concrete without steel fiber was prepared as a control mix. The engineering properties investigated in this study include workability, compressive strength, splitting tensile strength, flexural strength, direct tensile strength and stress-strain response under compressive axial load. The alkali-activated slag-fly ash concrete was cured under ambient conditions.

Table 2 shows the mix proportions of alkali-activated slag-fly ash concrete adopted from a previous study by Hadi et al. (2017). Ground granulated blast-furnace slag (GGBS) and Fly ash (FA) were used as binders for alkali-activated slag-fly ash concrete. A combination of sodium silicate (Na_2SiO_3) and sodium hydroxide (NaOH) was used as alkaline activators. Crushed aggregate with a maximum size of 10 mm and river sand were used as coarse and fine aggregates, respectively.

In this study, polyvinyl chloride (PVC) cylindrical molds of 100 mm × 200 mm were used for casting the alkali-activated slag-fly ash concrete specimens to measure the compressive strength according to AS 1012.9-1999 (AS 1999). In addition, polyvinyl chloride (PVC) cylindrical molds of 150 mm × 300 mm were used for casting the alkali-activated slag-fly ash concrete specimens to measure the splitting tensile strength and stress-strain response according to AS 1012.10-2000 (AS 2000) and AS 1012.17 (AS 2014), respectively. Plywood molds of 100 mm × 100 mm × 500 mm were used for casting alkali-activated slag-fly ash concrete specimens to measure the flexural strength and direct tensile strength. All alkali-activated slag-fly ash concrete specimens were cast in three layers and each layer was compacted for 10 seconds with an electric vibrator. After casting, the alkali-activated slag-fly ash concrete specimens were kept under ambient conditions at a temperature of 23 ± 3 °C and a relative humidity of 60 ± 10% for 24 hours. Afterwards, the specimens were removed from the mold and left under ambient conditions until the time of testing.

Labelling of alkali-activated slag-fly ash concrete mixes

In this study, each alkali-activated slag-fly ash concrete mix has been labelled with an acronym (Table 3). The symbols REF, ACMS, ACDS and ACHS refer to plain alkali-activated slag-fly ash concrete mix, alkali-activated slag-fly ash concrete mix with MS fibers, alkali-activated slag-fly ash concrete mix with DS fibers and alkali-activated slag-fly ash concrete mix with HS fibers, respectively. The numbers (1, 1.5, 2, and 3) afterwards refer to the percentages of steel fibers by volume used in alkali-activated slag-fly ash concrete mix. The ACHS mixes included 2% HS fibers by volume. The ACHS2a included 0.5% MS+1.5% DS fibers, ACHS2b included 1% MS+1% DS fibers and ACHS2c included 1.5% MS+0.5% DS fibers.

Test methods

Table 3 shows the test matrix for alkali-activated slag-fly ash concrete with and without steel fibers. All the specimens were tested in the Structural Engineering Laboratories at the University of Wollongong, Australia. For determining the consistency of the alkali-activated slag-fly ash mixes, slump tests were performed according to AS 1012.3.1-1998 (AS 1998).

The compressive strength tests of alkali-activated slag-fly ash concrete were conducted according to AS 1012.9-1999 (AS 1999) at 7 and 28 days. A compression testing machine with a capacity of 1800 kN was used to conduct the compressive strength tests. Before testing, the cylinders were capped with a high strength plaster to ensure uniform loading face. For each mix, three specimens were tested and the average compressive strengths have been reported.

The splitting tensile strength tests were performed according to AS 1012.10-2000 (AS 2000a) at 28 days. Two timber strips (5 mm thick × 25 mm wide × 400 mm long) were placed between the loading plate and the cylinder surface. A compression testing machine with a capacity of 1800 kN was used to conduct the splitting tensile tests. The specimens were tested at loading rate of 106 kN/min until the specimen failed. For each mix, three specimens were tested and the average splitting tensile strengths have been reported.

The flexural strength tests were performed under four-point bending according to AS 1012.11-2000 (AS 2000b) at 28 days. The prism specimens were tested under force controlled load applications at 2 kN/sec until the prism specimen failed. For each mix, three prism specimens were tested and the average flexural strengths have been reported.

Different test methods were used in the literature to measure the direct tensile strength of the concrete (Alhussainy et al. 2016). However, most of the test methods for direct tensile testing of concrete are associated with major drawbacks including load eccentricity, slippage and the fracture at the ends of the tested specimens. However, the test method developed in Alhussainy et al. (2016) was successful in overcoming the major drawbacks associated with the direct tensile testing of concrete. Hence, this test method was used to test the direct tensile strength of alkali-activated slag-fly ash concrete. The test was performed on alkali-activated slag-fly ash concrete prism specimens with a cross-section of 100 mm × 100 mm and a length of 500 mm. A wooden box, as shown in Fig. 2 was used as formwork for the specimens. To ensure failure in the middle of the specimen, the cross-sectional area of the specimen was reduced by using two timber triangular prisms with a height of 10 mm and a base of 20 mm. The triangular prisms were glued inside the wooden formwork vertically at the middle of the specimens, as shown in Fig. 2.

In order to apply the direct tensile force on the alkali-activated slag-fly ash concrete specimens, two steel gripping claws were embedded for 125 mm at both ends of the specimen. The gripping claws were made from a 20 mm diameter threaded steel bar which had four steel pins with 30 mm length and 8 mm diameter. These pins were welded to the threaded steel bar at 90 degrees with a spacing of 20 mm, as shown in Fig. 2.

To prevent any misalignment of the gripping claws and to ensure the application of the axial tensile loading during the testing, two universal joints were used. The universal joints were also used to hold the ends of specimens by the testing machine. Figure 3 shows the setup for direct tensile tests. All the specimens were tested using the 500 kN Universal Instron testing machine. The specimens were tested up to failure under a displacement controlled loading at 0.1 mm/min and the data were recorded at every two seconds.

In order to investigate the stress-strain response of the ambient cured alkali-activated slag-fly ash concrete mixes, tests were carried out according to the AS 1012.17 (AS 2014). The cylindrical specimens of 150 mm diameter and 300 mm height were tested in a 5000 kN Denison compression testing machine. At the middle half of the specimens, a standard compressometer with one linear variable differential transducer (LVDT) was used to measure the axial deformation of the specimens, while the axial load was obtained directly from the compression testing machine. The compression tests were performed under displacement controlled loads at 0.3 mm/min. To record the axial load and the corresponding axial deformation, an electronic data acquisition system was used. Before testing, the specimens of alkali-activated slag-fly ash concrete were capped with a high strength plaster to ensure uniform loading faces. Figure 4 shows the test arrangements for stress-strain response under compressive axial load.

Results and discussion

Ten alkali-activated slag-fly ash concrete mixes were designed to study the influence of different types of steel fibers on the engineering properties of ambient cured alkali-activated slag-fly ash concrete. The test results of alkali-activated slag-fly ash concrete mixes are reported in Table 4. The test results included the workability, compressive strength, splitting tensile strength, flexural strength, direct tensile strength and stress-strain response of ambient cured alkali-activated slag-fly ash concrete.

Workability

The slump test results are reported in Table 4. The addition of MS, DS, and HS fibers in alkali-activated slag-fly ash concrete mixes reduced the workability. The reduction in the workability increased with the increase in the volume fraction of different types of steel fibers in the ambient cured alkali-activated slag-fly ash concrete. Figure 5 shows the influences of different types of steel fibers on the workability of ambient cured alkali-activated slag-fly ash concrete.

Based on the test results, it can be found that the increase in the volume fraction of MS fibers from 0 (REF) to 3% (ACMS3), the slump of the ambient cured alkali-activated slag-fly ash concrete decreased by 35.6%. The slump for ACMS3 mix was only 76 mm. The ACMS3 mix was found to be difficult to cast and also the vibration during casting was not efficient. Therefore, some voids were observed when the specimens were de-molded. However, no flash set occurred during casting. It can also be observed that the increase in the volume fraction of DS fibers from 0 (REF) to 2% (ACDS2), the slump of the ambient cured alkali-activated slag-fly ash concrete decreased by 30.5%.

Finally, the addition of HS fibers exhibited a significant decrease in the slump of the ambient cured alkali-activated slag-fly ash concrete. The reduction in the slump was more for ACHS2a mix in which the reduction in the slump was 36.4% compared to the REF mix. From Fig. 5, it can be found that the trend for the decrease in the slump with an increase in the volume fraction of steel fibers was almost similar for all mixes. The decrease in the slump of the mixes with high steel fibers content could be attributed to the balling of steel fibers during the mixing process, which restrained the followability of the mixes.

Compressive Strength

The compressive strength of various mixes tested at 7 and 28 days are shown in Table 4. The compressive strength of ambient cured alkali-activated slag-fly ash concrete mixes was not significantly influenced by the addition of steel fibers, similar to the observations reported for OPC concrete (Bhargava et al. 2006; Ou et al. 2011). Figure 6 illustrates that the effect of the addition of different types of steel fibers on the compressive strength. The average compressive strength of the alkali-activated slag-fly ash concrete with steel fibers was slightly higher than the average compressive strength of alkali-activated slag-fly ash concrete without steel fibers. The alkali-activated slag-fly ash concrete without steel fiber (REF) achieved the average compressive strength of 40.1 MPa and 44.1 MPa on the 7 days and the 28 days, respectively.

It can be found that the increase in the volume fraction of MS and DS fibers from 0 to 2%, the compressive strength of ambient cured alkali-activated slag-fly ash concrete increased by 8.6% for ACMS2 mix and 4.1% for ACDS2 mix compared to the reference alkali-activated slag-fly ash concrete mix (REF). This increase could be attributed to the good distribution of steel fibers in alkali-activated slag-fly ash concrete mix which led to increasing in the bonding between the steel fibers and the alkali-activated slag-fly ash concrete mix and subsequently increased the compressive strength of alkali-activated slag-fly ash concrete. However, the compressive strength of alkali-activated slag-fly ash concrete decreased by 4.8% with the increase in the volume fraction of MS fiber from 2% (ACMS2) to 3% (ACMS3). The reduction in compressive strength was because of the reduction in the workability of the alkali-activated slag-fly ash concrete mix, as steel fibers created internal voids in alkali-activated slag-fly ash concrete. The internal voids were created due to insufficient vibration during casting. These voids reduced the density of alkali-activated slag-fly ash concrete, which resulted in a significant decrease in the compressive strength of alkali-activated slag-fly ash concrete. The optimum content of steel fiber that provided the maximum compressive strength was 2% for MS fibers and 2% for DS fibers.

Finally, the addition of HS fibers resulted in an increase in the compressive strength of ambient cured alkali-activated slag-fly ash concrete compared to the reference mix (REF). The improvement in the compressive strength of ACHS mix ranged from 4.5% to 10.8%. The highest compressive strength was achieved for the ACHS2b mix. The compressive strength of ACHS2b mix was 10.8% higher than the compressive strength of REF mix. The increase in the compressive strength was most likely because HS fibers with different sizes and shapes offered a combination of different restraint conditions. The micro steel fibers (MS) arrested the micro cracks and prevented the expansion of cracks. The DS fibers arrested the macro cracks and substantially improved the compressive strength of alkali-activated slag-fly ash concrete (Chen and Liu 2004).

Splitting tensile strength

The splitting tensile strengths of the ambient cured alkali-activated slag-fly ash concrete mix at 28 days are shown in Table 4. The experimental results demonstrated that the addition of steel fibers significantly influenced the splitting tensile strength of alkali-activated slag-fly ash concrete, similar to the observation reported for OPC concrete (Song et al. 2004; Yusof et al. 2011). Figure 7 shows the effect of the volume fraction of different types of steel fibers on the splitting tensile strength. It can be observed that the splitting tensile strengths of alkali-activated slag-fly ash concrete containing steel fibers were higher than the splitting tensile strength of alkali-activated slag-fly ash concrete without steel fibers. The average splitting tensile strength of REF mix was 3.50 MPa.

It can be seen that with the increase in the volume fraction of MS and DS fibers from 0 (REF) to 2%, the splitting tensile strength of alkali-activated slag-fly ash concrete increased by 51.4% for ACMS2 mix and 57.1% for ACDS2 mix. The increase in splitting tensile strength of alkali-activated slag-fly ash concrete can be attributed to the randomly oriented and the good distribution of steel fibers. Also, an increase in the bond strength between alkali-activated slag-fly ash concrete and steel fiber was achieved, which increased the splitting tensile strength of alkali-activated slag-fly ash concrete. However, increasing the volume fraction of MS fiber from 2% to 3% led to a decrease in the splitting tensile strength of alkali-activated slag-fly ash concrete by 9.2%. The decrease in the splitting tensile strength with the increase in the volume fraction of MS fibers from 2% to 3% was because the increase in the steel fiber increased voids in the alkali-activated slag-fly ash concrete. Consequently, the splitting tensile strength of alkali-activated slag-fly ash concrete decreased. The optimum volume fraction of steel fibers that provided the maximum splitting tensile strength was 2% for MS and 2% for DS fibers.

Finally, the addition of 2% HS fiber by volume increased the splitting tensile strength. The increase in the splitting tensile strength ranged between 48.6% and 80% compared to the reference alkali-activated slag-fly ash mix (REF). The highest splitting tensile strength of alkali-activated slag-fly ash concrete was achieved for ACHS2b mix. The splitting tensile strength of ACHS2b mix was 80% higher than the splitting tensile strength of REF mix.

Flexural strength

The flexural strengths of ambient cured alkali-activated slag-fly ash concrete at 28 days are shown in Table 4. The average flexural strength of ambient cured alkali-activated slag-fly ash concrete without steel fibers was 4.4 MPa. The experimental results illustrated that the addition of steel fibers significantly influenced the flexural strength of alkali-activated slag-fly ash concrete, similar to the observation reported for OPC concrete (Park et al. 2012; Kim et al. 2011; Yusof et al. 2011). Figure 8 shows the effect of the volume fraction of different types of steel fibers on the flexural strength of ambient cured alkali-activated slag-fly ash concrete. It can be observed that a significant increase in the flexural strength of alkali-activated slag-fly ash concrete was obtained by the addition of steel fibers.

It can be observed that for the increase in the volume fraction of MS and DS fiber from 0 (REF) to 2%, the flexural strength of alkali-activated slag-fly ash concrete increased by 22.7% for ACMS2 mix and 38.6% for ACDS2 mix. The increase in the flexural strength was attributed to the randomly oriented steel fibers crossing the cracked section, which resisted the propagation of micro and macro cracks. The arrest in the propagation of cracks increased the load-carrying capacity (Faisal and Ashour 1992). However, the increase in the volume fraction of MS fibers from 2% to 3%, the flexural strength decreased by 9.4%. The reason for the decrease in the flexural strength could be because the high volume fraction of steel fibers reduced the workability of the alkali-activated slag-fly ash concrete mix, which resulted in the nonhomogeneous distribution of steel fibers crossing the cracked section. The optimum volume fraction of steel fibers for the maximum flexural strength was 2% for MS and 2% for DS fibers.

Finally, the addition of 2% HS fibers by volume increased the flexural strength compared to the reference alkali-activated slag-fly ash concrete mix (REF). The improvement in the flexural strength of HS fibers reinforced alkali-activated slag-fly ash concrete ranged from

27.3% to 52.3% compared to REF alkali-activated slag-fly ash concrete mix. The highest flexural strength of alkali-activated slag-fly ash concrete obtained for the ACHS2b mix. The flexural strength of ACHS2b mix was 52.3% higher than the flexural strength of REF mix. This is because HS fibers with different sizes and shapes offered a combination of different restraint conditions. After test, a number of steel fibers crossing the cracked section were observed. The MIS fibers substantially influenced the bridging of micro cracks, while the DES fibers significantly influenced the bridging of macro cracks. Hence, greater efficiencies in delaying the growth of micro and macro cracks was achieved, which improved the flexural strength. Similar observations were reported in Sivakumar and Santhanam (2007) for high strength concrete reinforced with hybrid fibers.

Direct tensile test

Figure 9 shows the typical failure mode of ambient cured alkali-activated slag-fly ash concrete specimens with different types of steel fibers under direct tensile load. The failure of the reference plain alkali-activated slag-fly ash concrete mix (REF) occurred in a brittle manner with a complete fracture of the concrete specimens in the middle without prior signs of failure. On the other hand, the failure of all the specimens reinforced with 2% steel fibers (MS, DS and HS) by volume started with formation of cracks in the middle of the specimens. The presence of the steel fibers effectively prevented the sudden failure of alkali-activated slag-fly ash concrete specimens. As expected, the failures occurred in the middle of all the specimens as the cross section of the specimens was reduced by 20%. For all specimens tested under direct tensile load, no claw slippage was observed and no cracking occurred at the end of the specimens. This indicates that a proper alignment was achieved during testing.

The direct tensile strength was calculated as the maximum tensile load divided by the reduced cross-sectional area of the specimens (100 mm × 80 mm). Figure 10 shows the effect of the volume fraction of different types of steel fibers on the direct tensile strength of alkali-activated slag-fly ash concrete mix. It can be observed in Fig. 10 that the direct tensile strength is significantly increased by the addition of steel fibers compared to the direct tensile strength of plain alkali-activated slag-fly ash concrete mix (REF). It can be observed in Table 4 that the addition of 1%, 2% and 3% MS fibers by volume increased the direct tensile strength by about 8.3%, 20.8% and 16.6%, respectively, compared to the REF mix. The addition of 1%, 1.5% and 2% DS fibers by volume increased the direct tensile strength by 8.3%, 12.5% and 20.8%, respectively, compared to the REF mix. The addition of 2% HS fibers by volume significantly increased the direct tensile strength. The increase in the direct tensile strength ranged between 20.8% and 37.5% compared to the REF mix. The addition of 2% HS (1% MS and 1% DS) fiber by volume achieved the highest increase in the direct tensile strength. The increase in the direct tensile strength was about 37.5% compared to the REF mix. This is because high volume fraction of steel fibers with different sizes and shapes increased the availability of fibers crossing the cracked section. Hence, greater efficiency in delaying the growth of micro and macro cracks and the improvement in the direct tensile strength were achieved.

Stress-strain response under compressive axial load

The stress-strain response of ambient cured alkali-activated slag-fly ash concrete was determined by testing cylinder specimens with 150 mm in diameter and 300 mm in height. The stress-strain response of the cylinder specimens was evaluated at 28 days. The stress-strain curves of the specimens are shown in Fig. 11. It can be observed from Fig. 11 that the stress-strain response in both the ascending and descending branches of the curves were influenced by the addition of steel fibers. However, the most significant effect was noticed in the descending branch of the stress-strain curve. When the ascending branch of the stress-strain curves was almost linear until the peak axial load, the slope of the post-peak descending branch decreased significantly with the increase in the volume fraction of steel fibers. The addition of steel fibers to alkali-activated slag-fly ash concrete increased the peak stress and the strain corresponding to the peak stress. The increase in peak strain corresponding to the peak stress was more for mixes with higher volume fraction of steel fibers.

For the increase in the volume fraction of MS and DS fibers from 0 (REF) to 2%, the peak stress increased by 11.1% for the addition of 2% MS fibers by volume (ACMS2) and 5.9% for the addition of 2% DS fibers by volume (ACDS2) (Figure 11). However, increasing the MS fiber content from 2% to 3% by volume led to a reduction in the peak stress. This may be due to the high-volume fraction of steel fibers which led to a reduction in the workability of alkali-activated slag-fly ash concrete mix and resulted in a non-uniform distribution of the MS fibers during the mixing process. In addition, the high-volume fraction of steel fibers created voids in alkali-activated slag-fly ash concrete mixes.

The peak stress, strain corresponding to the peak stress and modulus of elasticity of the specimens are reported in Table 5. It was observed that the increase in the volume fraction of MS fibers from 0 (REF) to 3% (ACMS3), the strain corresponding to the peak stress increased by 57.1% (Table 5). It was also observed that the increase of DS fiber content from 0 (REF) to 2% (ACDS2), the strain corresponding to the peak stress in the alkali-activated slag-fly ash concrete increased by 42.8% (Table 5).

For HS fibers, the addition of 2% HS fibers by volume showed a significant influence on the stress-strain response compared to the reference mix (REF). The peak stress for alkali-activated slag-fly ash concrete with 2% HS fibers was higher than the peak stress of the reference mix (REF). The strain corresponding to the peak stress of alkali-activated slag-fly ash concrete was increased by 32.1%, 46.4%, and 35.7% for ACHS2a, ACHS2b, and ACHS2c, respectively compared to the reference mix (REF) (Table 5). It can also be observed that slopes of the descending branches (softening response) of the stress-strain curve for alkali-activated slag-fly ash concrete with HS fibers were very similar. The slope of the descending branches of the stress-strain response of the alkali-activated slag-fly ash concrete with HS fibers was significantly less steep than the slope of the reference mix (REF). This is because of the high-volume fraction of HS fibers in the alkali-activated slag-fly ash concrete mix. The presence of steel fibers in different mixed sizes and shapes improved the post-peak stress by bridging the small cracks at an early stage. At the beginning of macro cracking, the opening and growth of cracks were controlled by the bridging action of fibers. This mechanism increased the demand of energy for the cracks to propagate. Therefore, the improvement was achieved in the post-peak response of alkali-activated slag-fly ash concrete with HS fibers.

The area under the stress-strain curve represents to the toughness of the material. Figure 11 shows that the area under the stress-strain curve increased with the increase in the volume fraction of steel fibers, which indicated an increase in the toughness. The average toughness of the alkali-activated slag-fly ash concrete mixes was calculated and shown in Table 5. The limiting strain for the toughness was considered as 0.015, which is five times the ultimate concrete strain of 0.003 as specified in ACI 318-11 (ACI 2011) for conventional concrete. The toughness of different alkali-activated slag-fly ash concrete mixes was evaluated and the results are presented in Table 5. It can be seen from Table 5 the increase in the volume fraction of steel fibers led to a significant increase in the toughness of the alkali-activated slag-fly ash concrete. Similar to the observation reported for OPC concrete (Banthia et al. 2007; Yao et al. 2003). The highest improvement of the toughness of the alkali-activated slag-fly ash concrete was achieved for Mixes ACHS2b and ACHS2c. The toughness of Mixes ACHS2b and ACHS2c was approximately 400% higher than the toughness of REF. This may be because the concrete with different types and shapes of steel fiber provided a combined effect to the ability of fibers in arresting cracks at both micro and macro levels. Consequently, the toughness of alkali-activated slag-fly ash concrete increased.

Conclusion

This study evaluated the engineering properties of ambient cured alkali-activated slag-fly ash concrete mixes with different types of steel fibers i.e., micro-steel fibers (MS), deformed macro steel fibers (DS) and the combination of micro and deformed steel fibers, termed as hybrid steel fibers (HS). The engineering properties of ambient cured alkali-activated slag-fly ash concrete mixes were assessed in terms of a slump, compressive strength, splitting tensile strength, flexural strength, and direct tensile strength. The stress-strain response of ambient cured alkali-activated slag-fly ash concrete mixes with MS, DS and HS fibers was also investigated. The following conclusions are drawn from the test results presented in this study:

1. The addition up to 2% MS, DS, and HS fibers by volume in ambient cured alkali-activated slag-fly ash concrete mixes did not significantly affect the workability of alkali-activated slag-fly ash concrete mixes. However, the addition of 3% MS fibers by volume affected the workability of alkali-activated slag-fly ash concrete and led to less workable concrete.
2. The addition of 2% steel fibers (MS, DS and HS) by volume increased the compressive strength of ambient cured alkali-activated slag-fly ash concrete mixes. The highest compressive strength of alkali-activated slag-fly ash concrete was obtained for the addition of 2% HS (1% MS and 1% DS) fiber by volume in the alkali-activated slag-fly ash concrete

mixes. The increase in the compressive strength was about 10.8% compared to the reference alkali-activated slag-fly ash concrete mix (REF) without any fiber.

3. The splitting tensile strength and flexural strength of ambient cured alkali-activated slag-fly ash concrete mix significantly improved by the addition of MS, DS, and HS fibers. The addition of 2% HS (1% MS and 1% DS) fiber by volume achieved the highest splitting tensile strength and flexural strength. The increases in the splitting tensile strength and flexural strength were about 80% and 52.3% respectively, compared to the reference alkali-activated slag-fly ash mix (REF) without steel fiber.

4. The direct tensile strength of ambient cured alkali-activated slag-fly ash concrete increased with the increase in the addition of the volume fraction of steel fibers. The addition of 2% HS (1% MS and 1% DS) fiber by volume achieved the highest increase in the direct tensile strength. The increase in the direct tensile strength was about 37.5% compared to the reference alkali-activated slag-fly ash concrete mix (REF).

5. The addition of steel fibers into the ambient cured alkali-activated slag-fly ash concrete mixes changed the basic characteristics of the stress-strain response under axial compression. The ascending branch of the stress-strain curve was slightly influenced, but the descending branch (softening response) of the stress-strain curve was significantly influenced by the addition of steel fibers. The slope of the descending branch decreased significantly with the addition of steel fibers compared to the reference alkali-activated slag-fly ash concrete mix (REF).

6. The toughness of alkali-activated slag-fly ash concrete mixes increased with the increase in the volume fraction of steel fibers in the alkali-activated slag-fly ash concrete. The highest toughness was obtained by the addition of 2% HS (either 1% MS and 1% DS or 1.5% MS and 0.5% DS) fiber by volume in the alkali-activated slag-fly ash concrete mixes. The

additions of 2% HS (either 1% MS and 1% DS or 1.5% MS and 0.5% DS) fiber by volume achieved an increase in the toughness by 400% compared to the reference mix (REF).

Finally, the test results indicated that the addition of steel fiber improved the engineering properties of ambient cured alkali-activated slag-fly ash concrete mix. The highest improvement in the mechanical properties of the alkali-activated slag-fly ash concrete mix was achieved by the addition of 2% MS, 2% DS and 2% HS fibers by volume. The HS fiber reinforced alkali-activated slag-fly ash concrete mix with 1% MS and 1% DS fibers by volume achieved the optimum improvement in mechanical properties compared to the alkali-activated slag-fly ash concrete mix reinforced with other types of steel fibers.

Acknowledgments

The authors wish to express their gratitude to the technical officers at the High Bay Laboratory in the University of Wollongong, Australia for their help in carrying out the experimental work of this study. The authors are also thankful to Australian (Iron & Steel) Slag Association, Wollongong, Australia for providing aluminosilicate materials necessary for this study. In addition, the authors would like to acknowledge the Fibercon Company, Australia for providing deformed macro steel fibers required for this study. The first author wishes to thank the financial support for the full scholarship received from the Iraqi Government.

References

ACI (American Concrete Institute). (2011). "Building code requirements for structural concrete (ACI 318-11M) and commentary." *ACI 318-11M*, Farmington Hills, MI.

Al-Majidi, M. H., Lampropoulos, A., and Cundy, A. B. (2017). "Tensile properties of a novel fibre reinforced geopolymer composite with enhanced strain hardening characteristics." *Composite Structures*, 168, 402-427.

Alhussainy, F., Hasan, H. A., Rogic, S., Sheikh, M. N., and Hadi, M. N. S. (2016). “Direct tensile testing of self-compacting concrete.” *Construction and Building Materials*, 112, 903-906.

AS (Australian Standard). (1998). “Methods of testing concrete – method 9: determination of properties related to the consistency of concrete – slump test.” *AS 1012.3.1-1998*, Sydney, NSW, Australia.

AS (Australian Standard). (1999). “Methods of testing concrete. Method 9: Determination of the compressive strength of concrete specimens.” *AS 1012.9-1999*, Sydney, NSW, Australia.

AS (Australian Standard). (2000a). “Methods of testing concrete - Determination of indirect tensile strength of concrete cylinders (Brasil or splitting test).” *AS 1012.10-2000*, Sydney, R2014, NSW, Australia.

AS (Australian Standard). (2000b). “Methods of testing concrete - Determination of the modulus of rupture.” *AS 1012.11-2000*, Sydney, R2014, NSW, Australia.

AS (Australian Standard). (2014). “Methods of testing concrete - Determination of the static chord modulus of elasticity and Poisson’s ratio of concrete specimens.” *AS 1012.17-2014*, Sydney, NSW, Australia.

ASTM, C. 618 (2012). “Standard Specification for Coal Fly Ash and Raw or Calcined Natural Pozzolan for use as a Mineral Admixture in Portland Cement Concrete.” American Society for Testing of Materials, West Conshohocken, USA.

Australian Slag Association (2017). “Australasian Slag Association, Wollongong, NSW 2500.” <accessed on January 2017>, http://www.asa-inc.org.au/ground-granulated-blast-furnace-slag.php.

Bakharev, T., Sanjayan, J. G., and Cheng, Y.-B. (1999). “Alkali activation of Australian slag cements.” *Cement and Concrete Research*, 29(1), 113-120.

Bakharev, T., Sanjayan, J. G., and Cheng, Y.-B. (2003). “Resistance of alkali-activated slag concrete to acid attack.” *Cement and Concrete Research*, 33(10), 1607-1611.

Bakharev, T. (2005). “Durability of geopolymer materials in sodium and magnesium sulfate solutions.” *Cement and Concrete Research*, 35(6), 1233-1246.

Banthia, N., and Sappakittipakorn, M. (2007). “Toughness enhancement in steel fiber reinforced concrete through fiber hybridization.” *Cement and Concrete Research*, 37(9), 1366-1372.

Bernal, S., De Gutierrez, R., Delvasto, S., and Rodriguez, E. (2010). “Performance of an alkali-activated slag concrete reinforced with steel fibers.” *Construction and Building Materials*, 24(2), 208-214.

Bhargava, P., Sharma, U.K., and Kaushik, S.K. (2006). "Compressive stress-strain behavior of small scale steel fibre reinforced high strength concrete cylinders." *Journal of advanced concrete technology*, 4(1), 109-121.

Bhutta, A., Borges, P.H., Zanotti, C., Farooq, M. and Banthia, N. (2017). "Flexural behavior of geopolymer composites reinforced with steel and polypropylene macro fibers." *Cement and Concrete Composites*, *80*, 31-40.

Chen, B., and Liu, J. (2004). "Residual strength of hybrid-fiber-reinforced high-strength concrete after exposure to high temperatures." *Cement and Concrete Research*, 34(6), 1065-1069.

Davidovits, J. (1991). "Geopolymers: inorganic polymeric new materials." *Journal of Thermal Analysis and calorimetry*, 37(8), 1633-1656.

Duxson, P., Fernández-Jiménez, A., Provis, J. L., Lukey, G. C., Palomo, A., and Van Deventer, J. (2007). "Geopolymer technology: the current state of the art." *Journal of Materials Science*, 42(9), 2917-2933.

Eraring Australia (2017). **"**EPSA, Level 16, 227 Elizabeth Street Sydney NSW 2000.**"** < accessed on January 2017>, https://www.originenergy.com.au/about/ who-we- are/what-we-do/generation.html.

Faisal, F. W., and Ashour, S. A. (1992). "Mechanical properties of high-strength fiber reinforced concrete." *ACI Material Journal*, 89(5), 449-455.

Fernandez-Jimenez, A. M., Palomo, A., and Lopez-Hombrados, C. (2006). "Engineering properties of alkali-activated fly ash concrete." *ACI Materials Journal*, 103(2), 106.

Hadi, M. N. S., Farhan, N. A., and Sheikh, M. N. (2017). "Design of geopolymer concrete with GGBFS at ambient curing condition using Taguchi method." *Construction and Building Materials*, 140, 424-431.

Habert, G., De Lacaillerie, J. D. E., and Roussel, N. (2011). "An environmental evaluation of geopolymer based concrete production: reviewing current research trends." *Journal of cleaner production*, 19(11), 1229-1238.

Islam, A., Alengaram, U. J., Jumaat, M. Z., and Bashar, I. I. (2014). "The development of compressive strength of ground granulated blast furnace slag-palm oil fuel ash-fly ash based geopolymer mortar." *Materials & Design*, 56, 833-841.

Kim, D.J., Park, S.H., Ryu, G.S., and Koh, K.T. (2011). "Comparative flexural behavior of hybrid ultra-high performance fiber reinforced concrete with different macro fibers." *Construction and Building Materials*, *25*(11), 4144-4155.

Lokuge, W. and Karunasena, W. (2016). "Ductility enhancement of geopolymer concrete columns using fibre-reinforced polymer confinement." *Journal of Composite Materials*, 50**,** 1887-1896.

McLellan, B.C., Williams, R.P., Lay, J., Van Riessen, A., and Corder, G.D. (2011). “Costs and carbon emissions for geopolymer pastes in comparison to ordinary portland cement.” *Journal of Cleaner Production*, 19(9), 1080-1090.

Nath, P., and Sarker, P. K. (2014). “Effect of GGBFS on setting, workability and early strength properties of fly ash geopolymer concrete cured in ambient condition.” *Construction and Building Materials*, 66, 163-171.

Nataraja, M., Dhang, N., and Gupta, A. (1999). “Stress–strain curves for steel-fiber reinforced concrete under compression.” *Cement and concrete composites*, 21(5), 383-390.

Ng, T. S., Amin, A., and Foster, S. J. (2013). “The behaviour of steel-fibre-reinforced geopolymer concrete beams in shear.” *Magazine of Concrete Research*, 65(5), 308-318.

Olivia, M., and Nikraz, H. (2012). “Properties of fly ash geopolymer concrete designed by Taguchi method.” *Materials & Design*, 36, 191-198.

Ou, Y.C., Tsai, M.S., Liu, K.Y., and Chang, K.C. (2011). “Compressive behavior of steel-fiber-reinforced concrete with a high reinforcing index.” *Journal of Materials in Civil Engineering*, 24(2), 207-215.

Palomo, A., Grutzeck, M., and Blanco, M. (1999). “Alkali-activated fly ashes: a cement for the future.” *Cement and concrete research*, 29(8), 1323-1329.

Park, S.H., Kim, D.J., Ryu, G.S., and Koh, K.T. (2012). “Tensile behavior of ultra-high performance hybrid fiber reinforced concrete.” *Cement and Concrete Composites*, 34(2), 172-184.

Peng, J. X., Huang, L., Zhao, Y. B., Chen, P., and Zeng, L. (2013). “Modeling of carbon dioxide measurement on cement plants.” *In Advanced Materials Research,* 610, 2120-2128. Trans Tech Publications.

Ranjbar, N., Mehrali, M., Mehrali, M., Alengaram, U. J., and Jumaat, M. Z. (2015). “Graphene nanoplatelet-fly ash based geopolymer composites.” *Cement and Concrete Research*, 76, 222-231.

Ranjbar, N., Talebian, S., Mehrali, M., Kuenzel, C., Metselaar, H. S. C. and Jumaat, M. Z. (2016). “Mechanisms of interfacial bond in steel and polypropylene fiber reinforced geopolymer composites.” *Composites Science and Technology*,122, 73-81.

Rashad, A., Bai, Y., Basheer, P., Collier, N., and Milestone, N. (2012). “Chemical and mechanical stability of sodium sulfate activated slag after exposure to elevated temperature.” *Cement and Concrete Research*, 42(2), 333-343.

Roy, D. M., Jiang, W., and Silsbee, M. (2000). “Chloride diffusion in ordinary, blended, and alkali-activated cement pastes and its relation to other properties.” *Cement and Concrete Research*, 30(12), 1879-1884.

Ryu, G. S., Lee, Y. B., Koh, K. T., and Chung, Y. S. (2013). “The mechanical properties of fly ash-based geopolymer concrete with alkaline activators.” *Construction and Building Materials*, 47, 409-418.

Shaikh, F. U. A. (2013). “Review of mechanical properties of short fibre reinforced geopolymer composites.” *Construction and building materials*, 43, 37-49.

Sivakumar, A., and Santhanam, M. (2007). “Mechanical properties of high strength concrete reinforced with metallic and non-metallic fibres.” *Cement and Concrete Composites*, 29(8), 603-608.

Song, P. S., and Hwang, S. (2004). “Mechanical properties of high-strength steel fiber-reinforced concrete.” *Construction and Building Materials*, 18(9), 669-673.

Thomas, R. J., and Peethamparan, S. (2015). “Alkali-activated concrete: Engineering properties and stress–strain behavior.” *Construction and building materials*, 93, 49-56.

Yao, W., Li, J., and Wu, K. (2003). “Mechanical properties of hybrid fiber-reinforced concrete at low fiber volume fraction.” *Cement and concrete research*, 33(1), 27-30

Yip, C. K., Lukey, G. C., Provis, J. L., and van Deventer, J. S. (2008). “Effect of calcium silicate sources on geopolymerisation.” *Cement and Concrete Research*, 38(4), 554-564.

Yunsheng, Z., Wei, S., Zongjin, L., Xiangming, Z., and Chungkong, C. (2008). “Impact properties of geopolymer based extrudates incorporated with fly ash and PVA short fiber.” *Construction and Building Materials*, 22(3), 370-383.

Yusof, M. A., Nor, N.M., Zain, M.F.M., Peng, N.C., Ismail, A., Sohaimi, R.M., and Zaidi, A.M.A. (2011). “Mechanical properties of hybrid steel fibre reinforced concrete with different aspect ratio.” *Australian Journal of Basic and Applied Sciences*, *5*(7), 159-166.

List of Tables

List of Figures

Fig. 7. Average 28-days splitting tensile strength of ambient cured alkali-activated slag-fly ash concrete mixes (REF, ACMS, ACDS and ACHS)

Fig. 8. Average 28-day flexural strength of ambient cured alkali-activated slag-fly ash concrete mixes (REF, ACMS, ACDS and ACHS)

Fig. 9. Typical failure mode of ambient cured alkali-activated slag-fly ash concrete mixes under direct tension (REF, ACMS, ACDS, and ACHS)

Fig. 10. Average 28-day direct tensile strength of ambient cured alkali-activated slag-fly ash concrete mixes (REF, ACMS, ACDS and ACHS)

Fig. 11. Stress-strain response of ambient cured alkali-activated slag-fly ash concrete under axial compression: (a) ACMS, (b) ACDS and (c) ACHS

Table 1. Chemical composition (mass %) for GGBS (ASA 2017) and FA (EPSA 2017)

Component	SiO_2	Al_2O_3	Fe_2O_3	CaO	MgO	K_2O	Na_2O	TiO_2	P_2O_5	Mn_2O_3	SO_3	LOI*
GGBS	32.4	14.96	0.83	40.7	5.99	0.29	0.42	0.84	0.38	0.40	2.74	NA
FA	62.2	27.5	3.92	2.27	1.05	1.24	0.52	0.16	0.30	0.09	0.08	0.89

*LOI: Loss on ignition

Table 2. Mix proportions of ambient cured alkali-activated slag-fly ash concrete (Hadi et al. 2017)

Mix	Quantity
FA (kg/m^3)	225
GGBS (kg/m^3)	225
Al/Binder	0.35
Aggregate (kg/m^3)	1164
Sand (kg/m^3)	627

$Na_2SiO_3/NaOH$	2.5
Na_2SiO_3 (kg/m^3)	112.5
NaOH (kg/m^3)	45
NaOH (mole/l)	14
Superplasticizer (kg/m^3)	22.5
Water (kg/m^3)	45

Note: Al/Binder represents alkaline activator to binder content ratio.

Table 3. Test matrix

Alkali-activated concrete mix	Type of steel fiber	Percentage by volume
REF	Plain Concrete	-
ACMS1	Micro steel fiber (MS)	1%
ACMS2		2%
ACMS3		3%
ACDS1	Deformed steel fiber (DS)	1%

ACDS1.5		1.5%
ACDS2		2%
ACHS2a	Hybrid steel fiber (HS)	2% (0.5% MS+1.5% DS)
ACHS2b		2% (1% MS+1% DS)
ACHS2c		2% (1.5% MS+0.5% DS)

Table 4. Test results of ambient cured alkali-activated slag-fly ash concrete

Alkali-activated concrete mix	Slump (mm)	Compressive Strength (MPa) 7 days		Compressive Strength (MPa) 28 days		Splitting Tensile Strength (MPa)		Flexural Strength (MPa)		Direct Tensile Strength (MPa)	
		Average	S.D	Average	S.D	Average	S.D	Average	S.D	Average	S.D
REF	118	40.1	1.11	44.1	1.12	3.5	0.20	4.4	0.26	2.4	0.15
ACMS1	105	41.7	1.12	46.5	1.20	3.9	0.26	4.6	0.17	2.6	0.14
ACMS2	85	44.1	1.06	47.9	1.20	5.3	0.22	5.4	0.13	2.9	0.16
ACMS3	76	40.7	0.79	45.6	0.93	4.8	0.15	5.0	0.32	2.8	0.10
ACDS1	102	40.8	1.07	44.3	0.86	4.4	0.16	4.7	0.18	2.6	0.14
ACDS1.5	95	41.6	0.90	44.8	1.56	4.5	0.25	4.9	0.25	2.7	0.12
ACDS2	82	42.7	1.50	45.9	0.80	5.5	0.24	6.1	0.15	2.9	0.14
ACHS2a	75	42.2	1.26	46.1	1.39	5.2	0.19	5.6	0.24	2.9	0.15
ACHS2b	80	45.0	1.02	48.9	1.47	6.3	0.17	6.7	0.21	3.3	0.15
ACHS2c	82	42.7	1.59	46.6	0.98	5.6	0.16	5.9	0.21	3.0	0.18

Note: S.D represents standard deviation

Table 5. Axial stress-axial strain response of ambient cured alkali-activated slag-fly ash concrete under axial compression

Alkali-activated concrete mix	f'_{cf} (1)	ε'_{cf} (2)	Toughness	Toughness relative to the REF	Modulus of elasticity (GPa)
REF	42.4	0.0028	0.10	1	22.6
ACMS1	45.1	0.0033	0.36	3.6	24.7
ACMS2	47.1	0.0037	0.42	4.2	24.9
ACMS3	44.3	0.0044	0.48	4.8	23.9
ACDS1	42.5	0.0036	0.36	3.6	22.7
ACDS1.5	42.6	0.0039	0.42	4.2	22.8
ACDS2	44.9	0.0040	0.46	4.6	23.0
ACHS2a	45.7	0.0037	0.44	4.4	24.1
ACHS2b	48.0	0.0041	0.50	5.0	25.7
ACHS2c	44.9	0.0038	0.50	5.0	23.7

Note: (1) Average peak compressive stress in MPa. (2) Average strain corresponding to average peak stress.

(a) (b)

Fig. 1. Steel fibers: (a) MS fibers and (b) DS fibers

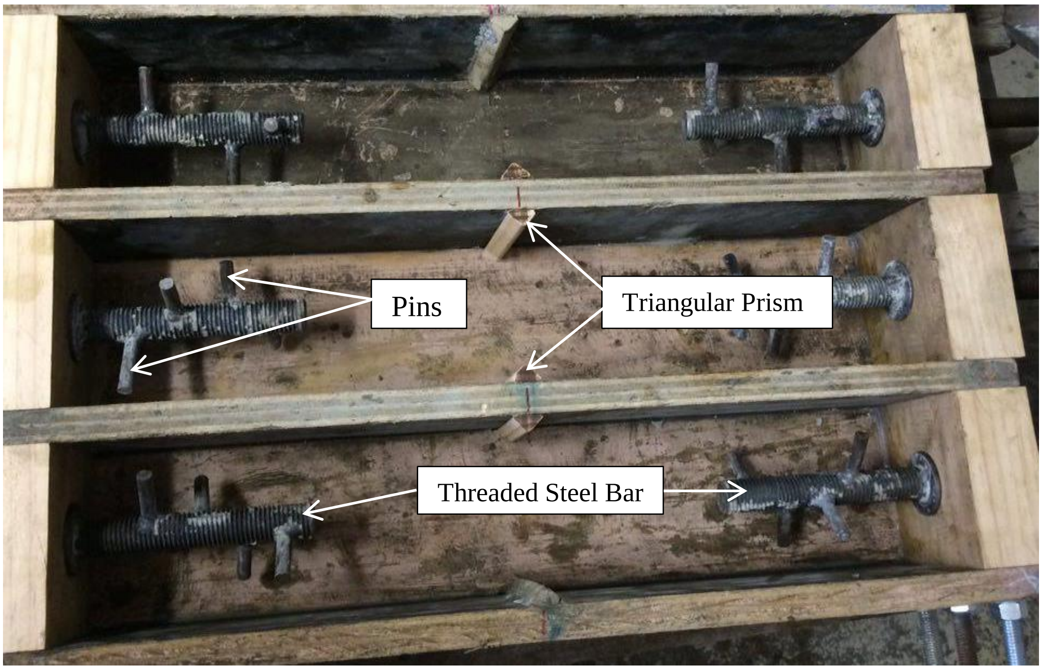

Fig. 2. Formwork of direct tensile test specimens

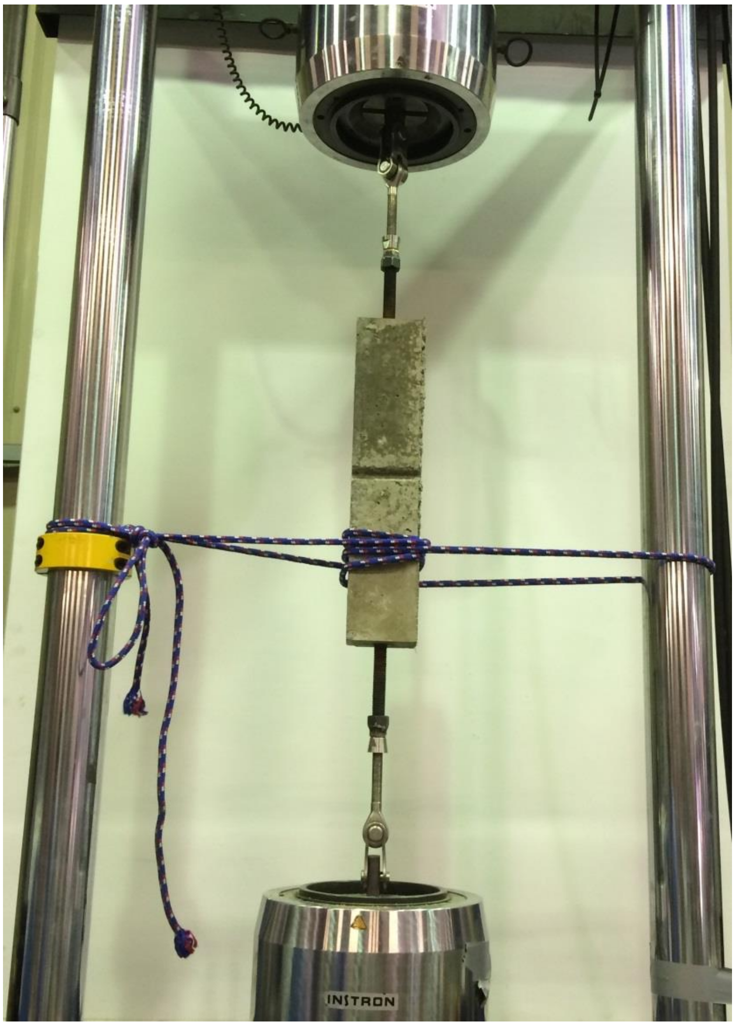

Fig. 3. Direct tensile testing setup

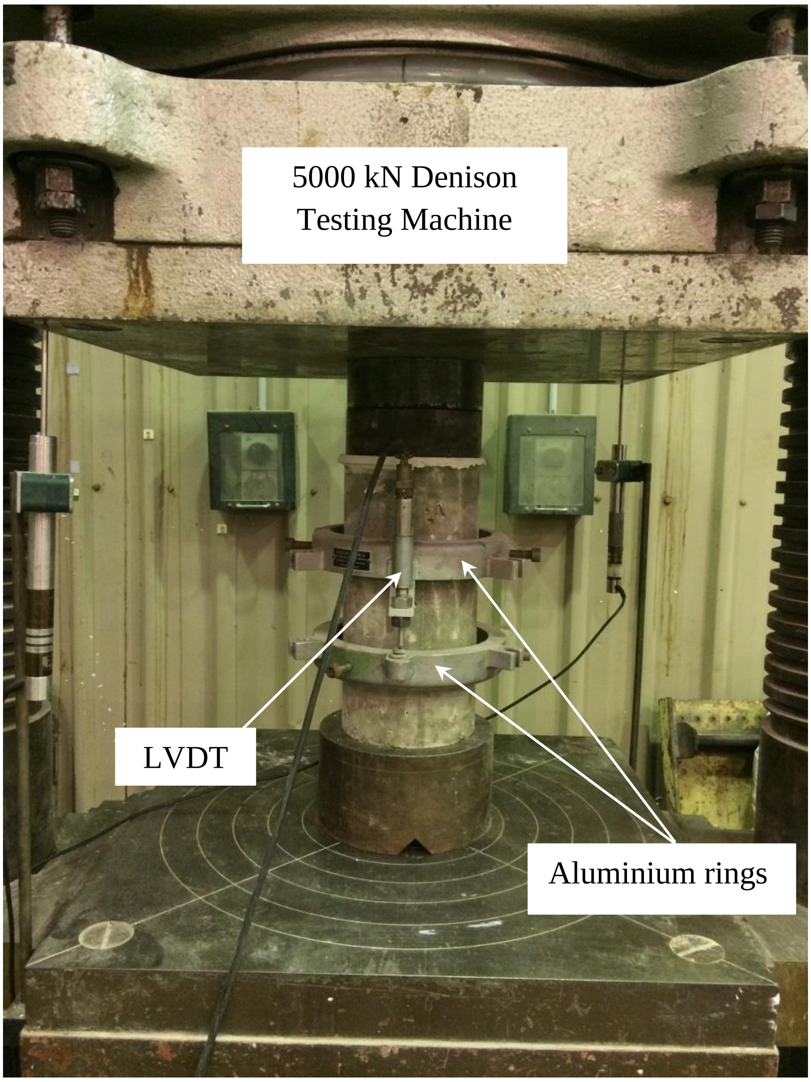

Fig. 4. Test setup for stress-strain response

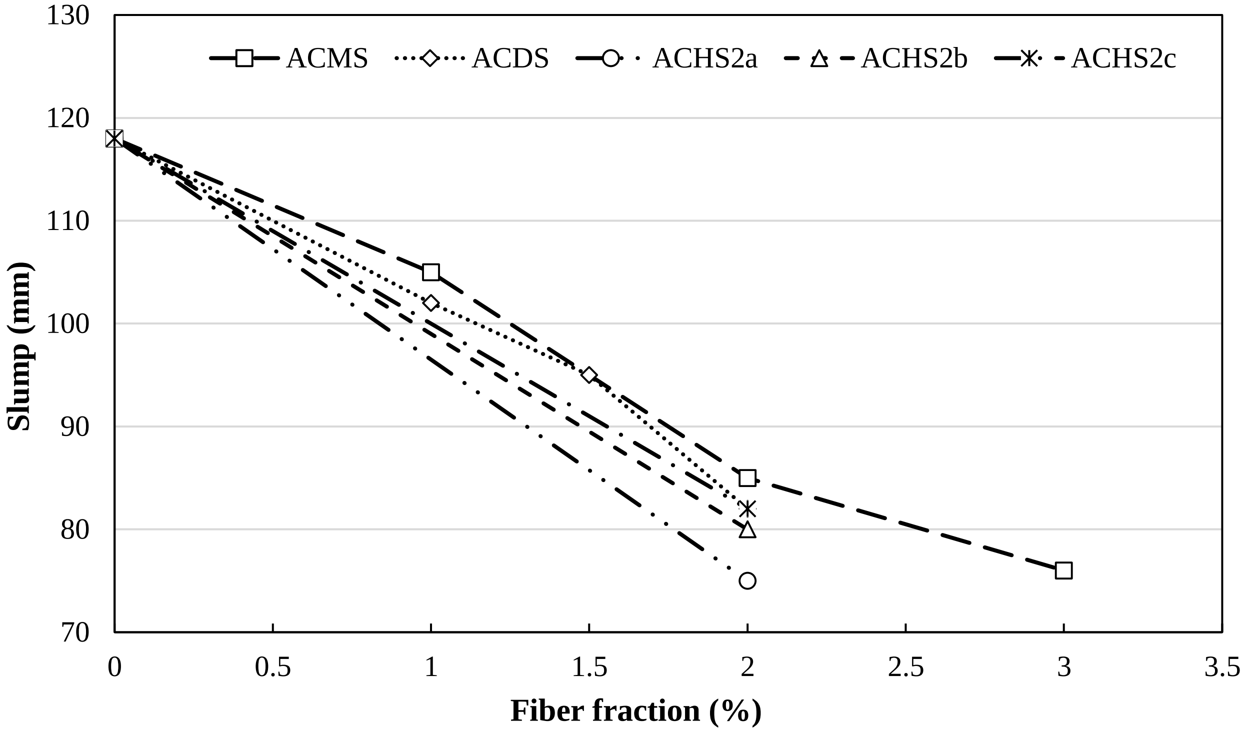

Fig. 5. Slump test results of alkali-activated slag-fly ash concrete mixes

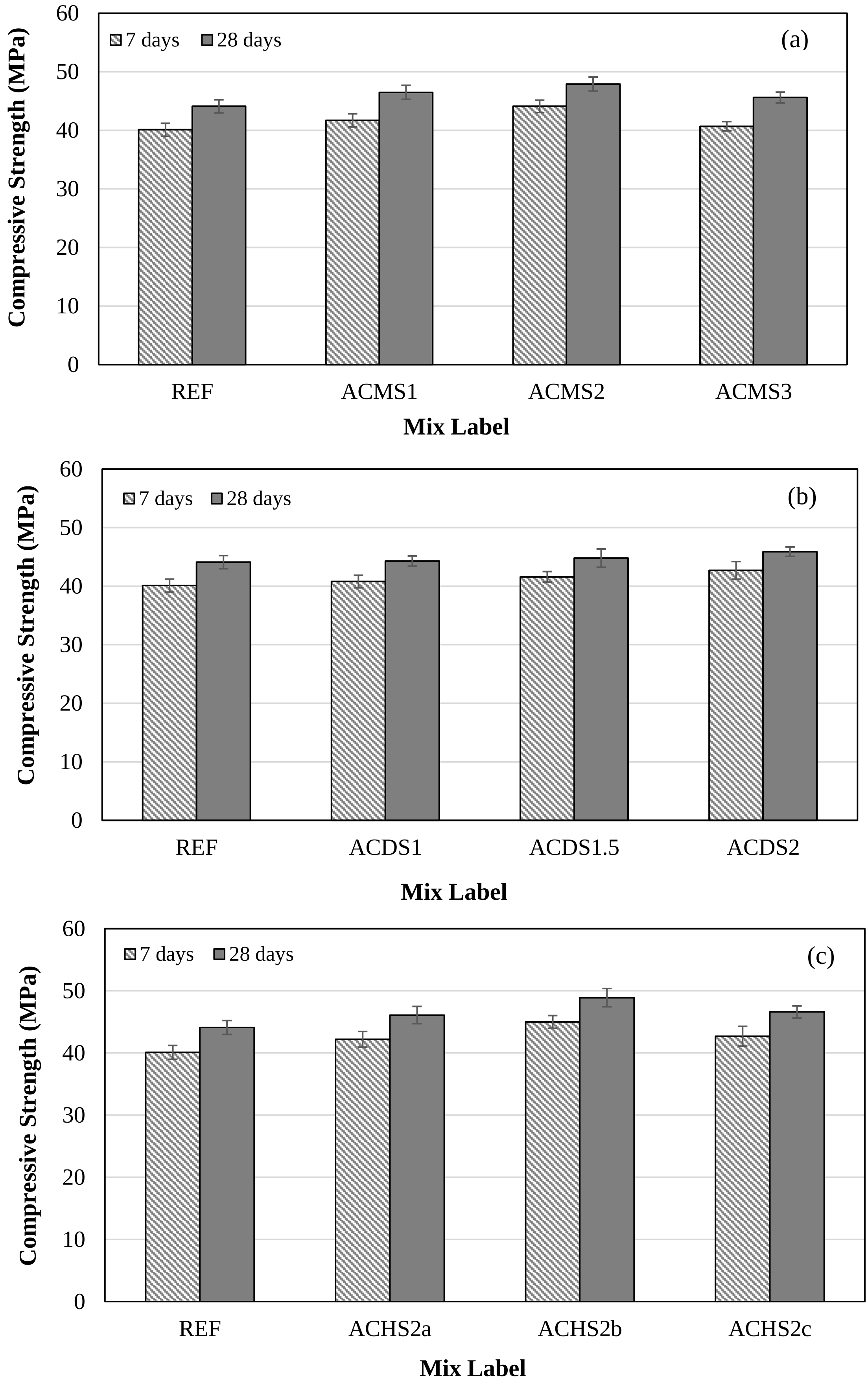

Fig. 6. Average compressive strength of ambient cured alkali-activated slag-fly ash concrete mixes: (a) ACMS, (b) ACDS and (c) ACHS

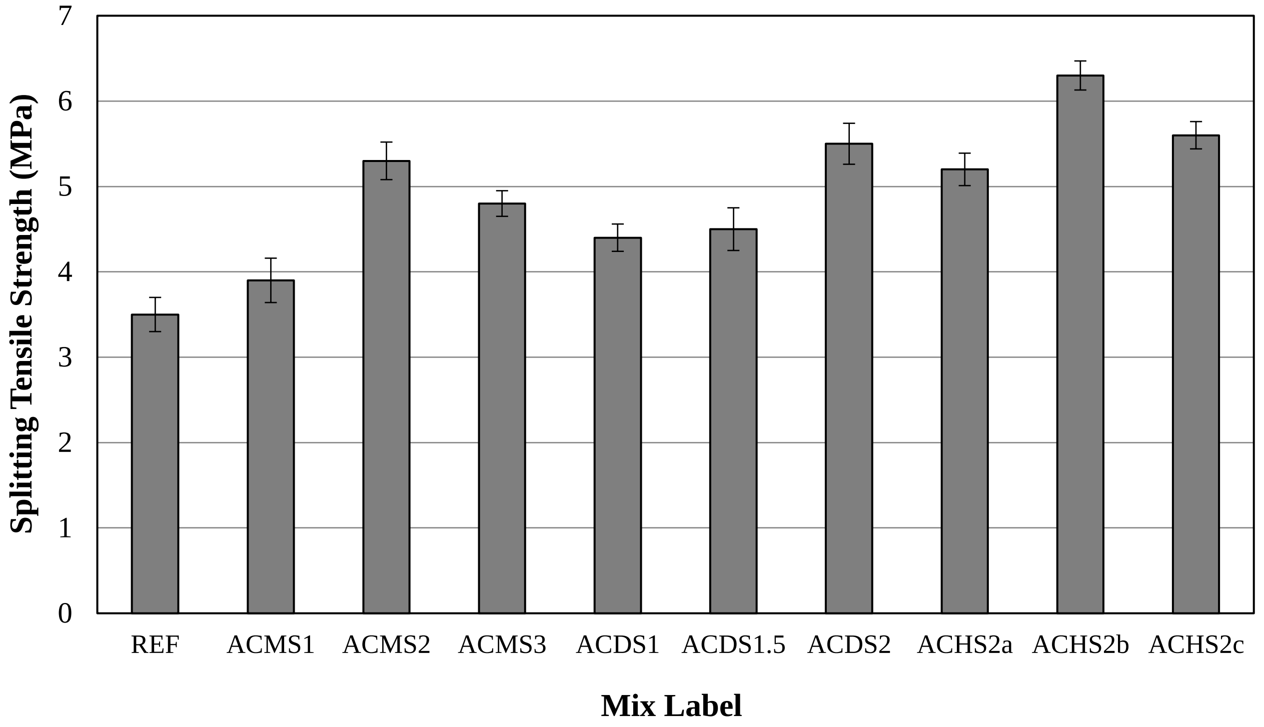

Fig. 7. Average 28-day splitting tensile strength of ambient cured alkali-activated slag-fly ash concrete mixes (REF, ACMS, ACDS and ACHS)

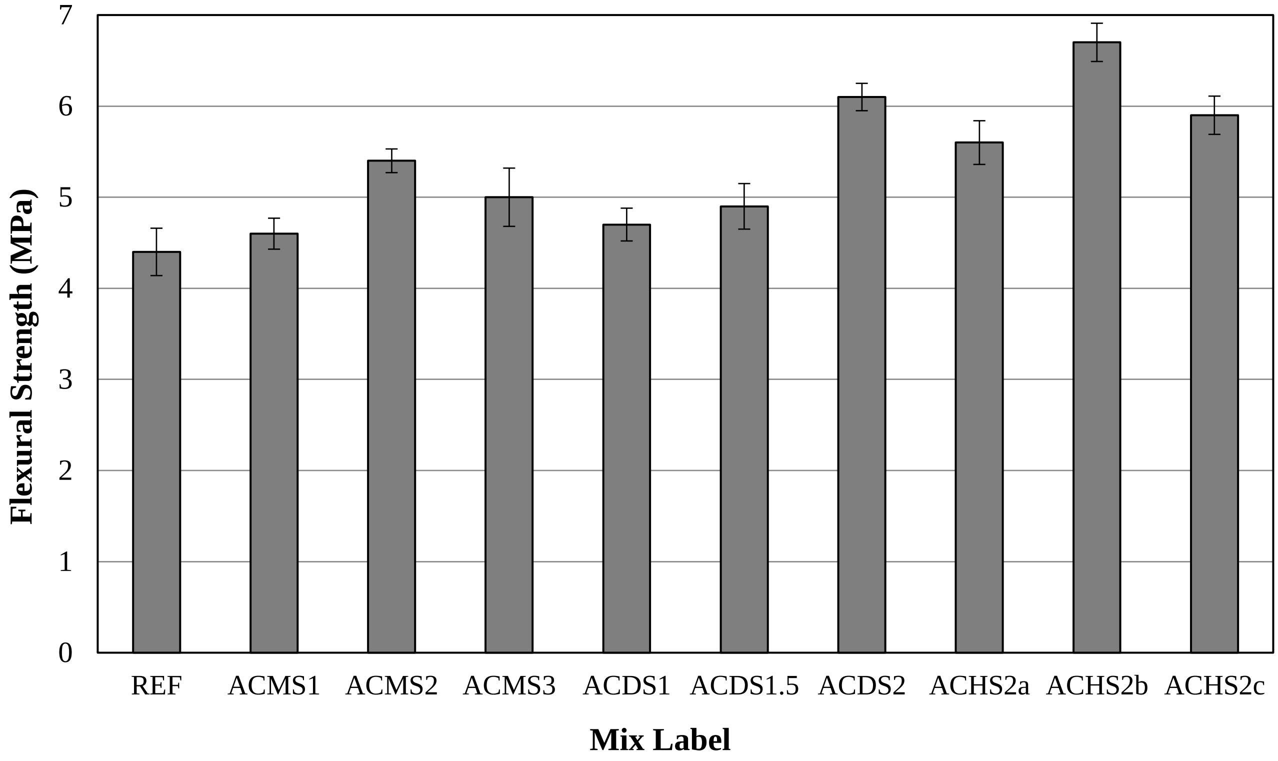

Fig. 8. Average 28-day flexural strength of ambient cured alkali-activated slag-fly ash concrete mixes (REF, ACMS, ACDS and ACHS)

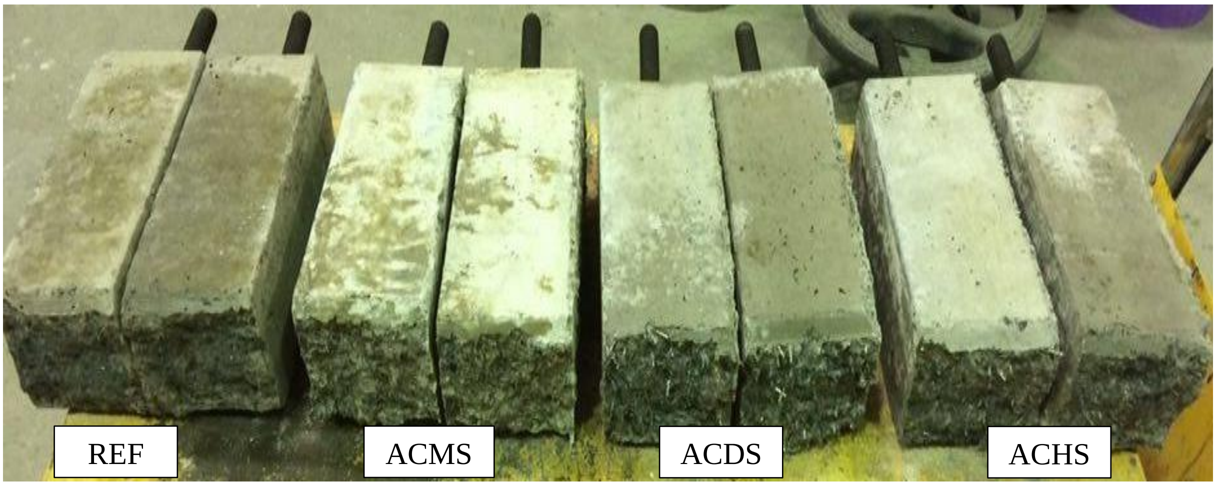

Fig. 9. Typical failure mode of ambient cured alkali-activated slag-fly ash concrete mixes under direct tension (REF, ACMS, ACDS, and ACHS)

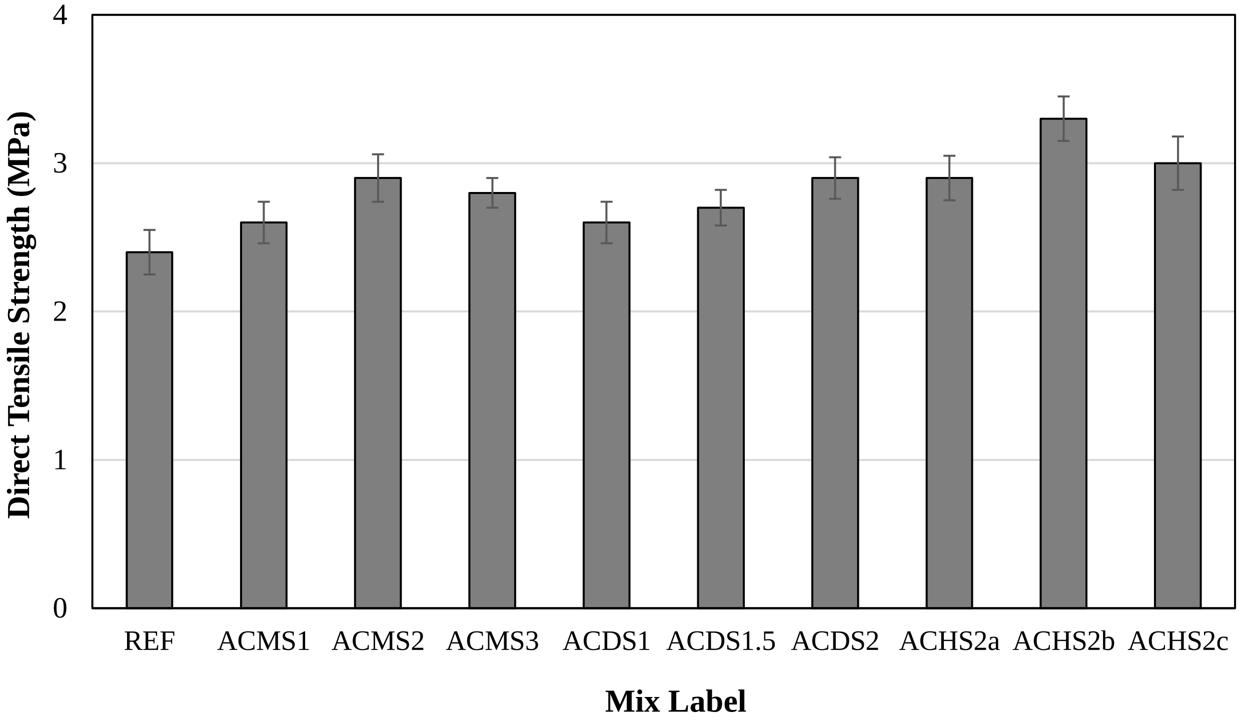

Fig. 10. Average 28-day direct tensile strength of ambient cured alkali-activated slag-fly ash concrete mixes (REF, ACMS, ACDS and ACHS)

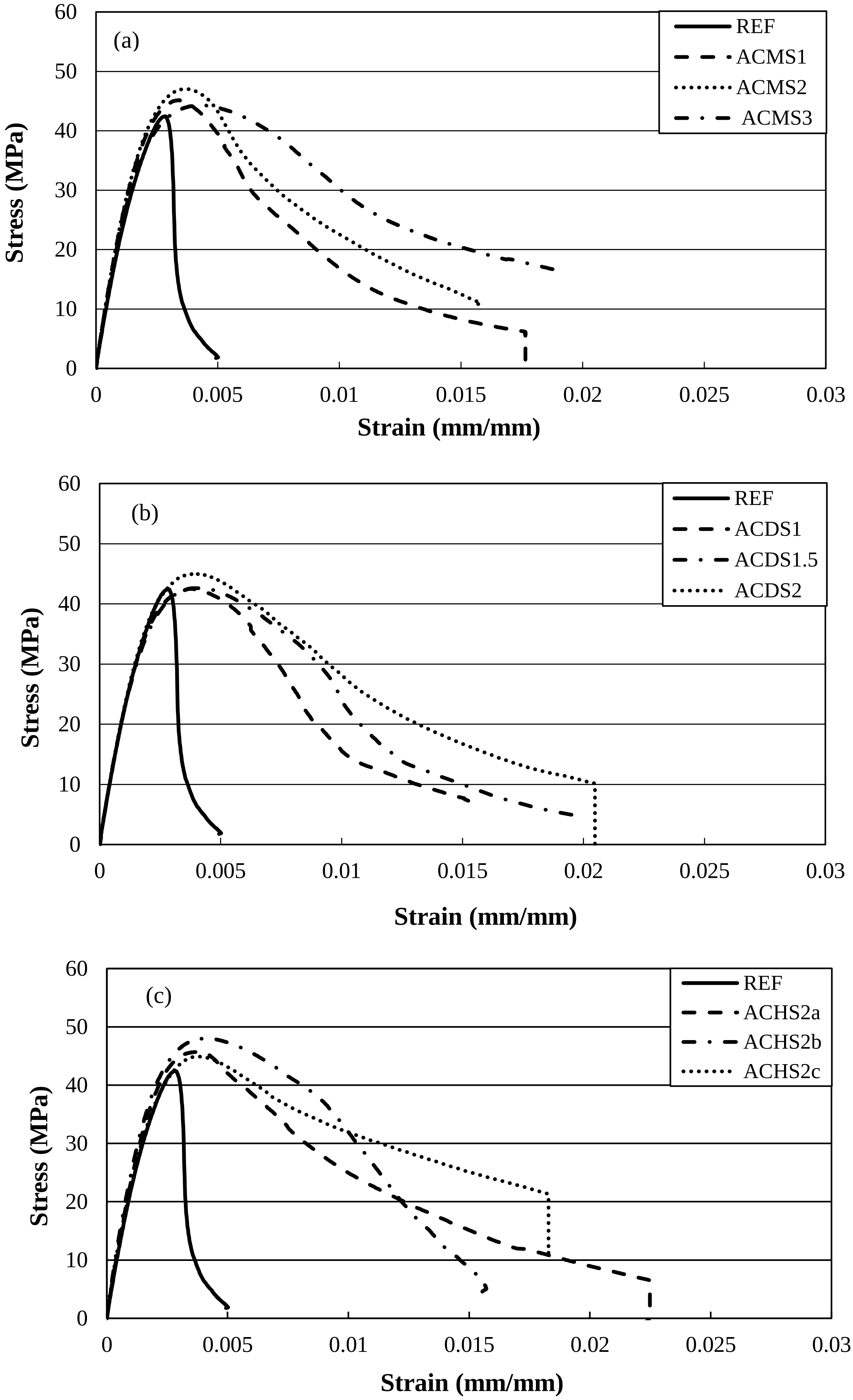

Fig. 11. Typical Stress-strain response of ambient cured alkali-activated slag-fly ash concrete under axial compression: (a) ACMS, (b) ACDS and (c) ACHS